

UNCLASSIFIED

Defense Technical Information Center
Compilation Part Notice

ADP023748

TITLE: Verification of Acoustic Propagation Over Natural and Synthetic Terrain

DISTRIBUTION: Approved for public release, distribution unlimited

This paper is part of the following report:

TITLE: Proceedings of the HPCMP Users Group Conference 2007. High Performance Computing Modernization Program: A Bridge to Future Defense held 18-21 June 2007 in Pittsburgh, Pennsylvania

To order the complete compilation report, use: ADA488707

The component part is provided here to allow users access to individually authored sections of proceedings, annals, symposia, etc. However, the component should be considered within the context of the overall compilation report and not as a stand-alone technical report.

The following component part numbers comprise the compilation report:

ADP023728 thru ADP023803

UNCLASSIFIED

Verification of Acoustic Propagation Over Natural and Synthetic Terrain

Harley H. Cudney, Stephen A. Ketcham, and Michael W. Parker

USACE Engineer Research and Development Center, Cold Regions Research and Engineering Laboratory (ERDC-CRREL), Hanover, NH

{Harley.H.Cudney, Stephen.A.Ketcham, Michael.W.Parker}@erdc.usace.army.mil

1. Introduction

Outdoor acoustic propagation is strongly affected by the covering over the ground, such as grass, snow, forest, or asphalt. To extend the usefulness of acoustic sensors to urban environments, we need to understand and accurately simulate how acoustic waves propagate in the presence of many reflective surfaces offered by buildings and man-made ground surfaces. Work by others modeling the physical mechanisms of how acoustic energy is absorbed by various materials is now coded into an acoustic propagation code and used to simulate how sound propagates over various types of terrain and infrastructure covered by a variety of materials.

2. Overview

In this paper we review the theoretical basis for the PSTOP3D acoustic propagation code and the recently-added features for acoustic source modeling and propagation over porous surfaces. We then present results from verification efforts for free-field propagation, propagation over porous surfaces, and comparison with experimental data for reflections from a wall. Finally, we review recent efforts to extend the modeling capabilities in the code, as well as continuing modeling efforts.

3. Description of PSTOP3D

Our computations are performed using a three-dimensional (3D) finite-difference time-domain (FDTD) code. The code suite is portable and is operational on several Department of Defense (DoD) High Performance Computing Modernization Program (HPCMP) machines, and is used to create high fidelity data sets of acoustic or seismic waves propagating over realistic terrain, and includes the ability to model buildings and infrastructure. For acoustics, the equations of motion and pressure are expressed in a rectangular variable-grid system and discretized with second-order differences. The

discretization scheme is staggered in time and space, allowing the use of an integration scheme known as the leapfrog approach^[1]. Properties at boundaries between layers are averaged using a scheme developed and demonstrated by Schröder and Scott^[2] to enhance stability across the boundaries of high-contrast materials.

The size (total number of grid nodes) of the models that can be run is proportional to the number of processors and memory available to each processor. The physical size of the model is proportional to the desired bandwidth of the acoustic response to be simulated. The run time is proportional to the length of time of the simulation. An example which was run on Sapphire (the Engineer Research and Development Major Shared Resource Center's [ERDC MSRC's] XT3, 2007 upgrade, with two cores per processor with two GB ram per core) is shown in Table 1. Resources required by PSTOP3D to run much larger acoustic models are listed in Parker, et al.^[3] Example resource requirements are shown in Table 1.

Table 1. PSTOP3D Resource Requirements

Parameter	Job 1	Job 2
Total nodes (millions)	1	257
Grid spacing (m)	0.25	0.25
Physical size (m)	25×25×25	288×88×88
Time step (s)	2500	1800
Number of cores	4	32
Wall time (s)	166	216,000

There are other methods for calculating the acoustic response over large scale terrain. These include ray-tracing methods^[4], finite-element modeling approach^[5], and the Fast Field Program^[6]. The advantage of the FDTD approach is it is very easy to mesh the problem domain, and algorithm is very simple. For simulating acoustic propagation requires only the implementation of these two relations (expanded to three-dimensions from two-dimension description in Wilson and Liu^[7]).

$$\frac{\partial p}{\partial t} = -\kappa_e \nabla v + \kappa_e Q \quad (1)$$

$$\frac{\partial v}{\partial t} = -\frac{1}{\rho_e} (\nabla p + \sigma v) \quad (2)$$

where p is the acoustic pressure, v is the vector of particle velocity components, t is time, κ_e is the effective bulk modulus in the material, ∇ is the divergence operator, ρ_e is the effective density of the medium, and σ is the static flow resistivity of the material (which is by definition zero for air, and nonzero for the porous materials used for ground and structures—this is described further in Section 5). In this form of the equations, the only input term, Q , represents a source idealized as a radially oscillating sphere^[8]. The units of the input are change in volume of the sphere per unit time per unit volume. We will say more about the source term in the next section.

The disadvantage of the FDTD approach is the program is computationally expensive, in that it requires node spacing of about 10 nodes per wavelength, and the response at every single node point in the domain is calculated before moving to the next time step. As a side note, the finite-element approach being developed as described in Reference 5 uses fewer elements per wavelength and may provide a more efficient approach.

The PSTOP3D program has been in use for several years at ERDC, and has been used to study acoustic and seismic propagation over realistic terrain^[9], tracking of vehicles^[10], detection of tunnels and underground facilities, and simulation of the effectiveness of sensors^[11]. The program has been used for private-sector customers under a Cooperative Research and Development Agreement (CRADA) and distributed—with accompanying training—to US Army Research and Development Engineering Center (ARDEC) for use in the Close Combat Support Systems. The program is undergoing continuously being improved in terms of ease of use, verification, validation, documentation, and incorporating the physics necessary to describe ever-more detailed propagation problems.

4. Acoustic Source Modeling

The only input term to Eqs. (1 and 2) is the source term Q . It is an idealized source in that it represents a sphere oscillating about some nominal radius with some velocity, affecting the surrounding medium equally in all directions^[8]. The radial vibration of the sphere serves to alternately compress and rarefy the medium, and this change in density corresponds to a change in pressure through the ideal gas law. However, the volumetric change per unit time per unit volume for various sources is not generally known. We typically measure changes in

pressure using microphones, but the measured changes in pressure are an *effect*, not a *cause*, of a physical process which creates sound. Treating measured pressure fluctuation as an input to the equations doesn't work from the point of view of the units of the equation, or from considerations of causality.

Nonetheless, we understand most sources in terms of the pressure fluctuations they cause. Pressure measured at a distance from a source can be modeled as a volumetric source through the relation^[5],

$$Q_s(t) = \frac{4\pi r}{\rho} \int p(t) dt \quad (3)$$

where $Q_s(t)$ is the required change in volume of the source per unit time which would cause the pressure fluctuations $p(t)$, and r is the distance of the pressure measurement from the source. Equation (3) has the units m^3/s , and is the total volumetric source. This equation provides a means of converting pressure measured at a distance to an ideal source, limited by the following two assumptions: 1) the source is modeled as acting at a point a distance r away from the measurement, and 2) the pressure measured at the distance r is assumed to be constant over a spherical surface of radius r .

Currently, PSTOP3D can accommodate multiple sources, but treats acoustic sources as acting at a single grid point. For the large-domain problems the grid spacing can be from 0.1 to 0.3 m, and the point source assumption is sufficiently accurate for many sources of interest (e.g., small-arms fire, small explosions). So the first assumption is not a severe limitation given our spatial scales and limited frequency range for large scale simulations. Furthermore, distributing the acoustic sources over a domain which reflects the size of the source would be straightforward.

The second assumption is more of a limitation. Many sources are measured in the free field, with the microphone often 1 m from the source. But most sources have some directivity, and the source power is characterized in general terms. The FDTD approach can accommodate sources with directivity, but the necessary free-field input data is not often available for large physical sources such as vehicles operating over terrain.

The ideal volumetric source $Q(t)$ which causes the measured pressure at the distance r must have the units $1/s$ to satisfy Eq. (1), and this means dividing the total required change in volume of the source per unit time by the volume over which the source is defined to get the change of volume per unit time per unit volume. In the FDTD approach, for a source acting at a single grid point, this means dividing by the unit volume at that grid point:

$$Q(t) = \frac{Q_s(t)}{dx \cdot dy \cdot dz} \quad (4)$$

where dx , dy , and dz are the dimensions of the cubo-id quadrilateral hexahedron (if dx , dy , and dz are equal, this is simply a cube).

5. Porous Surface Modeling

The term σv in Eq. (2) represents one effect of porosity. The effect of porous surfaces on acoustic propagation has been performed for 2D simulations, (Wilson, et al.^[12]), based on the work by Attenborough^[13,14]. We simply extend this to 3D and investigate constraints imposed by considerations of stability.

The physics of acoustic propagation in the free field is reflected in Eqs. (1 and 2), if term σ is zero. To include the effects of porous materials on acoustic propagation, the following parameters are used: the void fraction Ω (also called the material porosity, and is the volume of the pores per unit volume, m^3/m^3), static flow resistivity σ (which reflects the relative size of the pores, and which has the units $Pa/m^2/s$), and tortuosity, q , (no units) which reflects the geometry of the pores. These parameters were chosen as the simplest and most effective implementation of the extensive research on the effect of porosity on acoustic propagation. Wilson and Liu^[7] provide a convenient tabulation of these parameters tortuosity, porosity, and flow resistivity for asphalt, snow, sand, grass, and forest.

We have implemented equations for acoustic propagation for porous materials based on the following assumptions: (1) the pores are cylindrical, with the axial axis of the cylinder normal to the surface of the material, (2) our analysis is limited to relatively low frequencies (where the acoustic wavelengths are much larger than the pore dimensions), and (3) there is negligible temperature change due to the acoustic propagation, so isothermal relations apply).

To go from tortuosity and porosity to the effective bulk modulus and effective density, the following relations are used (limited to the assumptions above and modified slightly from Reference 7):

$$\kappa_e = \frac{\rho c^2}{\gamma \Omega} \quad (5)$$

$$\rho_e = \frac{4}{3} \frac{\rho q^2}{\Omega} \quad (6)$$

where γ is the ratio of specific heats of fluid portion of the porous material, c is the speed of sound in the fluid portion of the porous material, and ρ is the density of the fluid portion of the porous material.

The effect of porous materials are implemented in the preprocessor code portion of PSTOP3D in such a way that, during the high-performance computing processing,

Eqs. (1 and 2) are implemented across the whole computational domain. This is possible because the equations for porous materials are the same as single-state (e.g., all gas, all liquid, or all solid) if, in the preprocessor, the effective terms κ_e and ρ_e are set equivalent to κ and ρ , respectively, and the static flow resistivity is set to zero.

Our integration scheme is based on the necessary and sufficient condition for the size of the time step during integration to be bounded by the Courant condition. However, when highly reflective porous materials were implemented (e.g., asphalt), the simulations went unstable, and the instability started where the propagating wave first encountered the porous material. (Note, as mentioned previously, we have implemented the results from Reference 2 to maximize stability at an elastic interface). The results are explained if we examine the difference equation form of Eq. (2) used to update the particle velocity from the old time step to the next time step:

$$v_{new} = \left(1 - \frac{\Delta t}{\rho_e} \sigma \right) v_{old} - \frac{\Delta t}{\rho_e} \nabla p \quad (7)$$

where Δt is the time step(s). If we consider Eq. (7) as a finite-difference form of a first order equation in v (by taking ∇p to be constant over the time step), we recognize that for stability, the term $\left(1 - \frac{\Delta t}{\rho_e} \sigma \right)$ must be greater than zero.

We can meet this condition by limiting Δt , but materials such as asphalt have a static flow resistivity equal to $3e7 Pa/m^2/s$. Setting Δt to meet this condition would increase the computational cost by orders of magnitude.

We also investigated using central differences to approximate Eqs. (1 and 2); however, this approach requires more memory (to store the intermediate values of the fields for pressure and velocity; and this storage requirement triples in the seismic propagation simulations), and, although more stable than the Euler method implemented in PSTOP3D (in that it typically can use a larger time step and remain stable^[7]), there was still an onerous computational burden to implement the time step required for a stable solution. Please note that a specific condition for stability using the central difference approach was not derived.

The solution implemented that met both the resources- based requirement of using the Courant condition to set the time step, and the accuracy requirement for simulating over long distances, was to artificially cap the value of the static flow resistivity to satisfy,

$$\frac{\Delta t}{\rho_e} \sigma \leq 1 \quad (8)$$

The results show good agreement for asphalt, which is the most reflective of materials we implemented, and which is most significantly impacted by implementing Eq. (8). Equation (8) is the relationship that was used for simulations shown in References 3 and 11.

6. Ideal Free-field Propagation

The purpose of this verification is to ensure that simulations performed using PSTOP3D for propagation in the free-field agree with theory over distances up to 200 m, and that our modeling approach for modeling sources based on a measured pressure yields the exact measured pressure at the same distance from the source.

A small simulation for examining the source used a 40 Hz harmonic pulse source located in the geometric center of a model 100 nodes on each side, with an absorbing layer of 10 nodes on all six sides, using a cosine-based grid stretching formula with an amplitude of 4, and the model being completely composed of air with an acoustic wave speed of 347 m/s and a density of 1.2 kg/m³. To show that the results are independent of grid spacing, two different grid spacings are used, 0.25 and 0.1 m, with corresponding integration time steps of 0.414 and 0.165 ms, respectively. The results are shown in Figure 1, and the acoustic source term generates the required pressure amplitude of 1 Pa at 1 m from the source.

A larger simulation was run using a grid of 1280 × 448 × 448 nodes, with a grid spacing of 0.25 m, with a harmonic source located 44 m away from five boundaries. The air properties and the absorbing layer are the same as the previous example. The sinusoidal harmonic is analytically integrated to give a cosine function, offset to start at 0 m³/m³/s, and filtered to avoid starting transients for the higher-frequency inputs. The filtered input signal is shown in Figure 2 for the 40 Hz harmonic input, and the results compared to theory for transmission loss in air are shown in Figures 3 and 4, for harmonic sources at 40 and 100 Hz, respectively. Note that the definition for sound transmission loss is,

$$TL = 20 \log_{10}[p(x)/p(x=1m)] \quad (9)$$

where $p(x)$ is the root-mean-square of the pressure amplitude. The theory for pressure amplitude as a function of distance from the source is,

$$|p_{theory}| = \frac{|p(x=1m)|}{x} \quad (10)$$

The results show excellent agreement, with errors building up to less than 1 dB 200 m from the source for the 100 Hz harmonic input.

7. Propagation over Porous Layers

Initial results comparing propagation over porous layers is shown in Figure 5. The parameters of the problem are shown in Table 2. The Fast Field Program has been extensively verified and tested for propagation over porous materials. Note that the model capped the static flow resistivity in a slightly different way.

Table 2. Problem parameters for verifying accuracy of propagation due to asphalt

Parameter	Value
Grid	1,400 x 1,400 x 580
Spacing (m)	0.25
Domain (unstretched, m)	350 x 350 x 145
Absorbing region	20 elements, scale factor = 4
Time step (ms)	0.414
Pressure @ 1 m from source (Pa)	1.0
Source location – three different heights (m)	x = 150.2, y = 177.2, z=[24.2; 27.9; 42.9]
Frequency (Hz)	50, 100 Hz
Receiver locations – three different heights, extended series in x (m)	150.2 + 0.5 m*400 points, 177.2, [24.2; 30.2; 45.2]
Ground height (m)	21.9

8. Response Due to an Explosion

Based on an experiment by Albert & Liu^[15], we have an analytical model which closely approximates the pressure from a high-order explosion of a single block of C4. The equation for the pulse is,

$$p(t) = \left(1 - 16[150 \cdot t - 0.25]^2\right) e^{-10(150 \cdot t)/3} \quad (11)$$

The results are shown in Figure 6.

9. Summary

By modeling pressure using an idealized oscillating sphere, we can reproduce the exact pressure measured in the free field. Due to the computational costs required to meet the stability constraints we are forced to artificially limit the static flow resistivity, however, comparison to the Fast Field Program for asphalt (which has the highest static flow resistivity in the group of materials for which we have values), we see the predicted reflectivity has very little error when compared to an ideal rigid (i.e., completely reflective) surface.

Further work will extend the verification effort to other materials, validate the code by comparing to experimental data, and develop a method to model an ideal source based on pressure measurements which are not completely in the free-field.

Acknowledgements

Funding support is from DoD HPCMP Software Applications Institute I-01: Institute for Maneuverability and Terrain Physics Simulation; USACRREL 6.2 Program "URBAN Seismic/Acoustic Signatures and Phenomenology;" and CRREL 6.2 T14 program "Collecting and Modeling Acoustic Signatures for Mortars, Shoulder-Fired Rockets, and UAV's". Computational support is from HPCMP Project ERDCH11304ERD. The authors acknowledge experimental data and technical support from Dr. Donald G. Albert, ERDC – Hanover.

References

- Ostashev, V.E., D.K. Wilson, L. Liu, D.F. Aldridge, N.P. Symons, and D. Marlin, "Equations for finitedifference, time-domain simulation of sound propagation in moving inhomogeneous media and numerical implementation." *J. Acoust. Soc. Am.*, 117 (2), pp. 503–517, 2005.
- Schröder, C.T. and W.R. Scott, Jr., "On the Stability of the FDTD Algorithm for Elastic Media at a Material Interface." *IEEE Trans. Geoscience and Remote Sensing*, 40 (2), pp. 474–481, 2002.
- Parker, M.W., S.A. Ketcham, H.H. Cudney, and D.G. Albert, "Acoustic Wave Propagation in Urban Environments." *Proc. HPCMP Users Group Conference*, DoD High Performance Computing Modernization Program, 18–22 June, Pittsburgh, PA, IEEE Computing Society, 2007, to appear.
- Wilson, D.K., R. Bey-Hernandez, and V.E. Ostashev, "Statistical Models for Fading and Coherence of Sound in Urban Environments." *J. Acoust. Soc. Am.*, 120 (5, Pt. 2), pp. 3336–3337, 2006.
- Dey, S. and D. K. Datta, "A parallel hp-FEM infrastructure for three-dimensional structural acoustics." *Intl. J. for Numer. Methods Engineering*, John Wiley & Sons, 68, pp. 583–603, 2006.
- Wilson, D.K., "Sensor Performance Evaluator for Battlefield Environments (SPEBE) Tutorial." *US Army ERDC-CRREL Technical Report TR-06-12*, 2006.
- Wilson, D.K. and L. Liu, "Finite-Difference, Time- Domain Simulation of Sound Propagation in a Dynamic Atmosphere." *US Army ERDC-CRREL Technical Report TR-04-12*, 2004.
- Pierce, A.D., *Acoustics: "An Introduction to its physical principles and applications."* *Acoust. Soc. of Am.*, Melville, NY, p. 159, 1994.
- Ketcham, S.A., J. Lacombe, T.S. Anderson, and M.L. Moran, "Seismic Propagation from Humans in Open and Urban

Terrain." *Proc. HPCMP Users Group Conference*, DoD High Performance Computing Modernization Program, IEEE Computer Society, pp. 270–277, 2005.

10. Ketcham, S.A., M.L. Moran, J. Lacombe, R.J. Greenfield, and T.S. Anderson, "Seismic source model for moving vehicles." *Trans. Geosc. Rem. Sens.*, IEEE. 43, pp. 248–256, 2005.

11. Ketcham, S.A., D.K. Wilson, H.H. Cudney, and M.W. Parker, "Spatial Processing of Urban Acoustic Wave Fields from High-Performance Computations." *Proc. HPCMP Users Group Conference*, DoD High Performance Computing Modernization Program, 18–22 June, Pittsburgh, PA, IEEE Computing Society, 2007, to appear.

12. Wilson, D.K., V.E. Ostashev, S.L. Collier, N.P. Symons, D.F. Aldridge, and D.H. Marlin, "Time-domain calculations of sound interactions with outdoor ground surfaces." *Applied Acoustics*, Elsevier, New York, NY, 68 (2), pp. 173–200.

13. Attenborough, K., "Acoustical Characteristics of rigid fibrous absorbents and granular materials." *J. Acoust. Soc. Am.*, Melville, NY, 73, pp. 785–799.

14. Attenborough, K., "Acoustical Impedance Models for Outdoor Ground Surfaces." *J. Sound and Vibration*, Academic Press, New York, NY, 99 (4), pp. 521–544

15. Liu and, L. and D.G. Albert, "Acoustic pulse propagation near a right angle wall." *J. Acoust. Soc. Am.*, 119 (4), pp. 2073–2083, 2006.

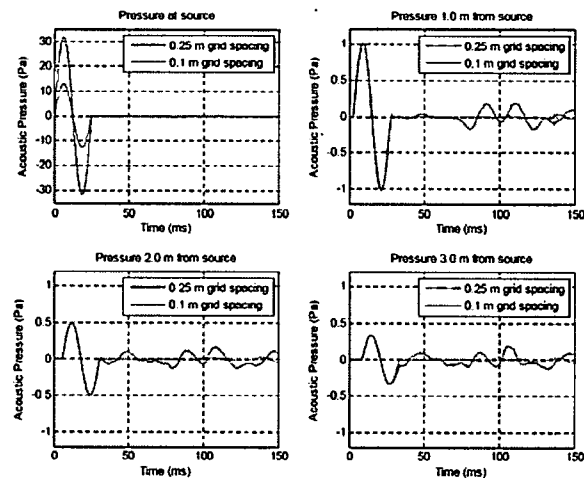


Figure 1. Response to 40 Hz harmonic pulse

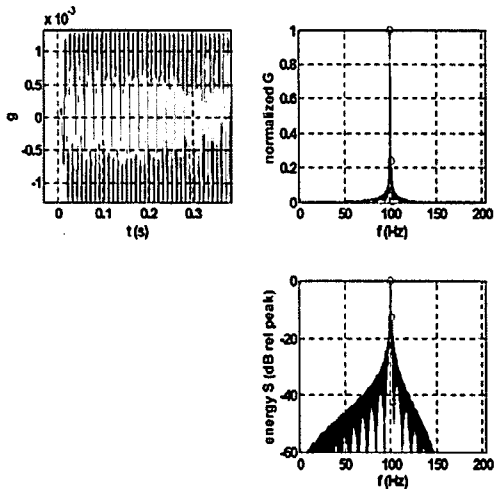


Figure 2. Input $Q(t) = 100$ Hz sine wave, after integration and low-pass filtering

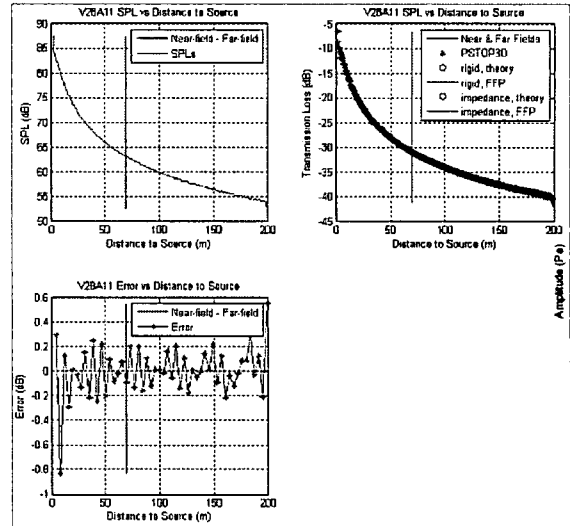


Figure 5. Reflectivity of asphalt calculated by PSTOP3D and Fast Field Program, compared to propagation over an ideal rigid surface

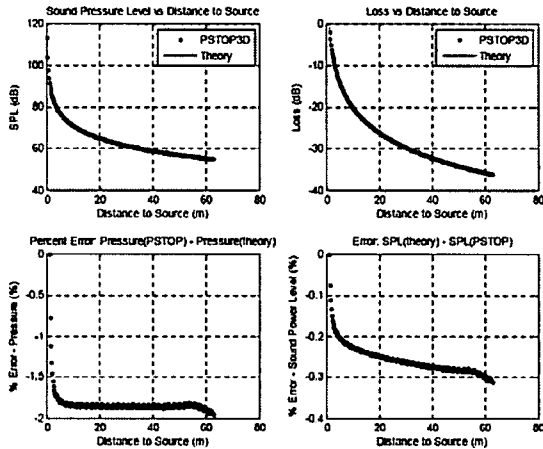


Figure 3. Comparison of PSTOP3D to Fast Field Program, 40 Hz harmonic input

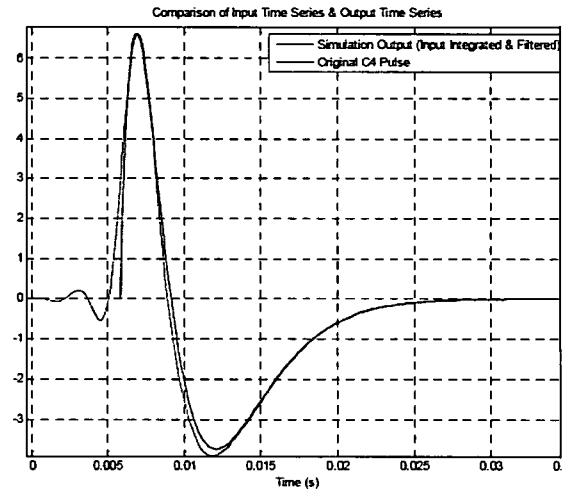


Figure 6. Comparison of output from PSTOP3D with original pulse. (Original pulse shifted to account for delay introduced by filtering).

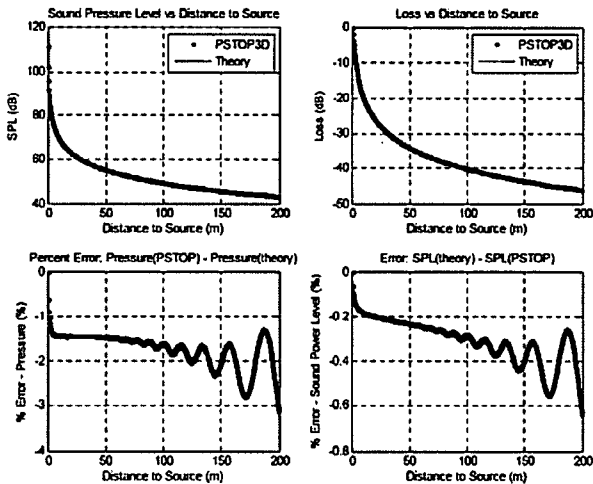


Figure 4. Comparison of PSTOP3D to Fast Field Program, 100 Hz harmonic input